Korean J. Chem. Eng., 39(4), 833-837 (2022)
DOI: 10.1007/s11814-022-1059-6

pISSN: 0256-1115
eISSN: 1975-7220

RAPID COMMUNICATION

Facile construction of acid-resistant Au nanoclusters via hydrophobic carbon coating for catalyzing CO oxidation in acidic media

Hao Wang, Hong Liu, and Jiasheng Wang†

School of Chemical Engineering, Dalian University of Technology, Panjin 124221, China
(*Received 6 October 2021 • Revised 9 December 2021 • Accepted 2 January 2022*)

Abstract−The oxidation of CO in acidic media is very important. For example, in direct methanol fuel cell, CO tends to poison the Pt electrode and cause a reduction of cell output power. CO can be removed by oxidation under the catalysis of Au nanoclusters with an optimal size of 2 nm. However, such small Au clusters tend to be corroded in the acidic media. Here we developed a facile method to solve this problem via hydrophobic carbon coating. The Au@C composite was prepared by reverse microemulsion-hydrothermal method. The hydrophobic carbon can effectively avoid the corrosion of gold nanoclusters by an acid environment while catalyzing CO oxidation efficiently.

Keywords: Au Nanocluster Catalyst, Hydrophobic Carbon Coating, Acid-resistant, CO Oxidation, Reverse Microemulsion

With the continuous acceleration of energy consumption in decades, mankind is facing severe energy crisis and environmental protection issue [1]. Direct methanol fuel cell (DMFC) has attracted much attention because of its merits of high energy density, low cost, and cleanliness [2,3]. At present, many efforts have been put to find the best performance of DMFC [4-6].

As the simplest monohydric alcohol, methanol has three C-H bonds, one C-O bond, and one O-H bond. In methanol oxidation process, the C-H bond and O-H bond are easier to be broken than the C-O bond, so CO will be generated [7], especially when pure Pt is used as the anode electrode [8]. The produced carbon monoxide is always adsorbed on the Pt electrode, which hinders the catalytic effect of Pt on methanol oxidation and finally causes a reduction of cell output power. A plausible method to remove CO is oxidation to CO_2 with the help of a powerful catalyst.

Gold, the most inert metal, has been used as the traditional currency for thousands of years. However, in 1987, Haruta et al. discovered that Au loading on oxide support shows high activity in catalyzing CO oxidation when its size is less than 10 nm, which changes the people's perception of Au, and since then has opened an entirely new chapter in the study [9]. Besides, the price of Au is slightly lower than that of Pt group metals and shows higher low-temperature CO catalytic oxidation activity. It is not affected by air humidity and CO concentration. Through the catalytic oxidation test of CO on this series of catalysts of different sizes, it was found that when the Au particle size was about 2 nm, it showed the highest catalytic activity [10].

Meanwhile, in the strong acidic media currently used in DMFC, acid-resistant CO oxidation catalysts are needed. Gold is generally considered to be acid-resistant. However, when the size of the metal approaches a metal cluster (2 nm), its properties such as catalytic performance, optical performance, magnetic properties, and metallic properties will change pronouncedly. Wu et al. found that when the metal size is small to a certain limit, relatively labile metals can be reduced by relatively inert metals. They proved it with practical experiments and named it as anti-galvanic reaction (AGR) [11]. So small-sized Au can not only replace metal ions that are more active than it [12-15], but also can chemically react with acetic acid, which means that Au clusters can be corroded by acid [16]. Therefore, developing acid-resistant Au nanoclusters has become a very meaningful research for catalyzing CO oxidation.

In this study, we used carbon to wrap the Au nanoclusters because carbon is a hydrophobic material, resistant to acid corrosion, and can prevent the hydrogen ions from accessing the metal active center. Thus the hydrophobic carbon can effectively avoid the corrosion of gold by the acid environment in DMFC while removing CO by catalytic oxidation.

The Au@C catalyst was prepared through a reverse microemulsion-hydrothermal method [17]. Reverse microemulsion is a thermodynamically stable "nanoreactor" which can be used to synthesize small-sized nanomaterials [18-23]. In a typical experiment, 7.6 g of polyoxyethylene (5) nonylphenyl ether (NP-5), 0.5 mL of aqueous ammonia, 0.5 mL of deionized water were dissolved in 20 mL of cyclohexane, and the mixture was stirred to form transparent reverse microemulsion. 0.28 mL of formaldehyde, 20 μL of $HAuCl_4$ and 0.22 g of para-aminophenol (4-AP) were added in to the reverse microemulsion with continually stirring. The mixture solution was stirred at 25 °C for 12 h and transferred into a Teflon-lined autoclave hydrothermally aged at 100 °C for another 12 h. The resulting products were collected by centrifugation (6,000-8,000 rpm, 10 min), washed with deionized water and ethanol, and dried at 60 °C for 10 h. The Au@amino phenolic formaldehyde resin polymer spheres were obtained (denoted as Au@APF). Au@C was then obtained by calcining Au@APF at 650 °C with a heating rate of 5 °C/min and holding them at that temperature for 3 h under a N_2 atmosphere. Au@C(RF) was prepared for comparison according to the

†To whom correspondence should be addressed.
E-mail: jswang@dlut.edu.cn

same procedure above except using resorcinol instead of 4-AP to get resorcinol formaldehyde resin (RF). $Au@SiO_2$ was also prepared for comparison according to the same procedure above except using TEOS instead of 4-AP and formaldehyde.

Scheme 1 shows the formation process of Au@C composite material. The reverse microemulsion system is composed of NP-5, aqueous ammonia, deionized water, and cyclohexane. After stirring, a uniform and stable reverse microemulsion was formed. Then chloroauric acid solution, formaldehyde, and 4-AP were added successively. The subsequent hydrothermal treatment can accelerate the further polymerization of the APF polymer [24]. In the first two hours, only some irregular polymer cores can be formed due to the slow reaction of the phenolic resin, at which time the Au is reduced by formaldehyde. After 2-6 hours of reaction, the product polymerizes into balls, and the APF polymer increases after 6-12 hours. In this process, formaldehyde and 4-AP polymerized on the Au surface and coated more Au during the polymerization and cross-linking process. The amino group of the APF can increase the force between Au and the support. After the carbonization, APF polymer was converted into carbon in an inert environment, and Au nanoclusters were encapsulated in situ.

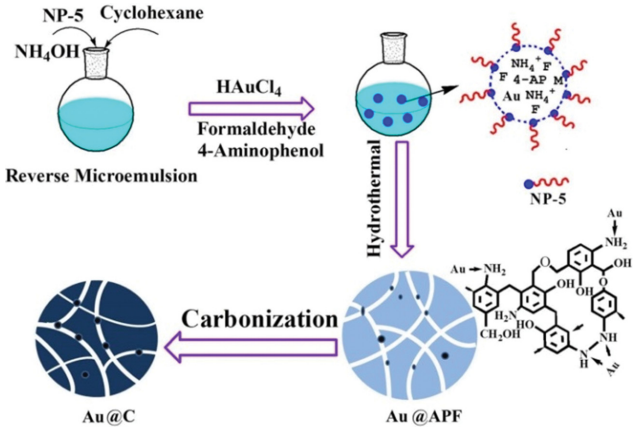

Scheme 1. The schematic illustration for the synthesis of Au@APF and Au@C using the reverse microemulsion-hydrothermal method.

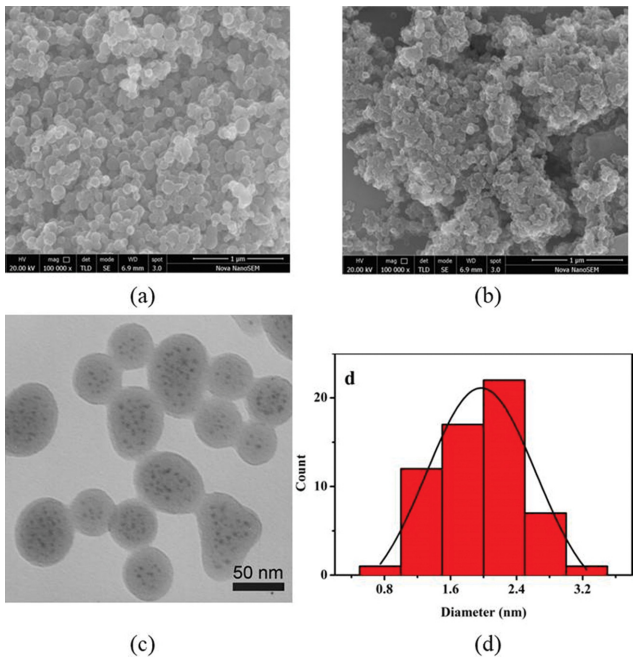

Fig. 1. (a) SEM image of Au@APF, (b) SEM image of Au@C, (c) TEM images of Au@C, and (d) the corresponding size distribution histogram of the Au clusters.

Fig. 1(a) and Fig. 1(b) show the SEM images of Au@APF and Au@C, respectively. It can be seen that the Au@APF composite material is about 100 nm. After conversion to Au@C, the size is greatly decreased to about 80 nm. Pyrolysis leads to ~20% shrinkage from Au@APF polymer to Au@C, which is consistent with the result reported before [17].

Fig. 1(c) and Fig. 1(d) are the TEM image of Au@C and the corresponding size distribution histogram of the Au clusters, respectively. As we can see, Au has a diameter of about 2 nm and is evenly distributed in carbon spheres. We used 4-AP as the raw material of carbon instead of resorcinol as we reported before [17]. The purpose is to introduce amino groups, because Au has a strong coordination interaction with amino groups. Therefore, the interaction between the metal and carbon nanospheres can be enhanced. When resorcinol-formaldehyde (RF) polymer was used as the carbon precursor, a serious aggregation happened to the gold particles according to TEM images (Fig. 2). The activity of Au with larger size is lower, which is not conducive to be used as a good catalyst for CO oxidation. Besides, Au cannot be well encapsulated in carbon converted from RF because the attraction between gold and carbon is too weak. This again demonstrates the importance of amino modification, which we have illustrated before [25,26].

The specific surface area of Au@C is 500 m^2/g, calculated from the nitrogen sorption isotherm (Fig. 3(a)). Fig. 3(b) shows the pore size distribution calculated by HK model, confirming the presence of micropore of 0.7 nm. Such a pore size is big enough for the CO/O_2/CO_2 molecules to get in and out. At the same time, Au clusters can be well protected and cannot escape.

The acid resistance of Au@C composite material was studied, and $Au@SiO_2$ with a hydrophilic support was compared (Scheme 2). Typically, a certain amount of composite material was weighed and dispersed into 5 mL of concentrated hydrochloric acid (theo-

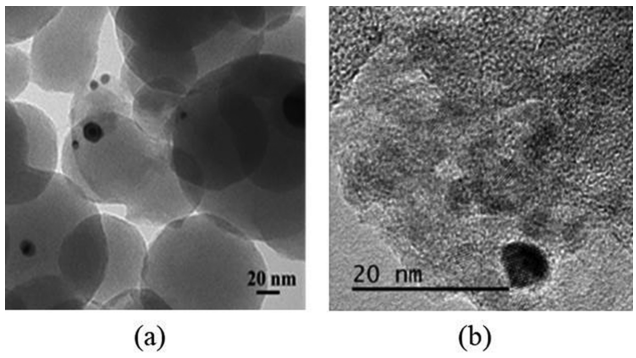

Fig. 2. TEM images of Au@C(RF) converted from Au@RF. (a) and (b) show different magnifications.

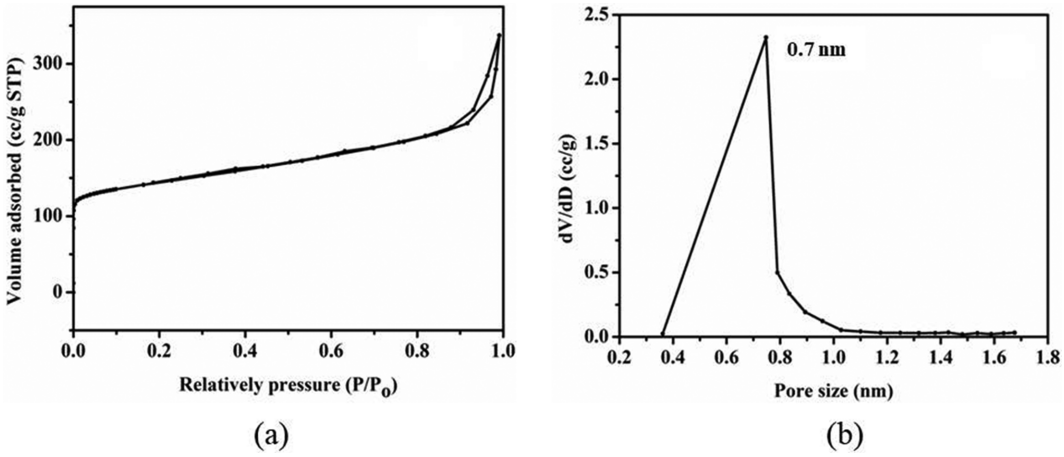

Fig. 3. (a) N_2 adsorption-desorption isotherms and (b) the micropore size distribution of Au@C.

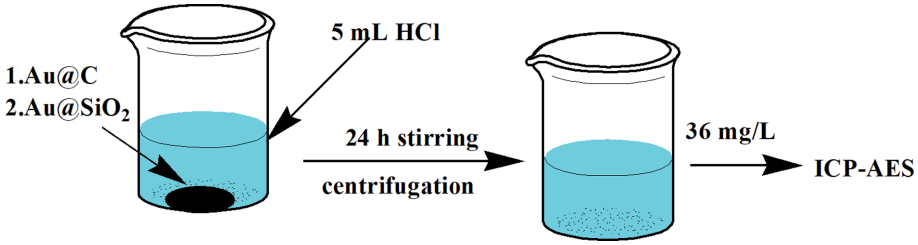

Scheme 2. Acid resistance test of Au@C and Au@SiO_2 composites.

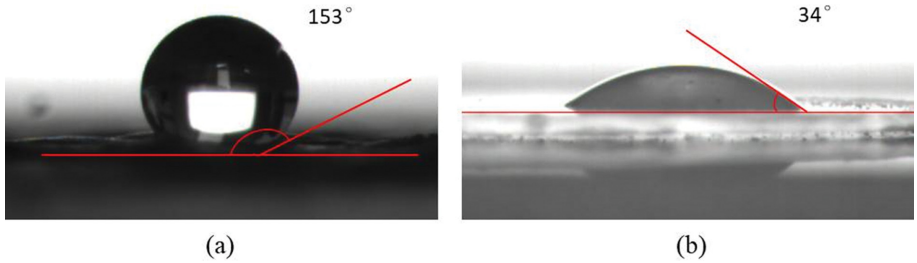

Fig. 4. The contact angle of (a) Au@C and (b) Au@SiO_2.

retically, if all the Au is dissolved, the concentration of Au in hydrochloric acid solution is 36.5 mg/L). After soaking for 24 h, solid was removed through centrifugation to get the clear solution, labeled as sample 1 for Au@C and sample 2 for Au@SiO_2, respectively. Then, the Au concentration was studied by an inductively coupled plasma atomic emission spectrometry (ICP-AES, PerkinElmer, Optima 2000 DV). Test showed that the concentration of Au in sample 1 was 0.0387 mg/L, and that in sample 2 was 3.791 mg/L. Thus, the loss of Au in Au@C composites soaked in hydrochloric acid was only about 0.11%, while the loss of Au in Au@SiO_2 soaked in hydrochloric acid was about 10.4%. A significant difference can be observed between the hydrophobic support and the hydrophilic support.

To explore the cause of corrosion resistance, contact angle was tested. As shown in Fig. 4, the contact angles for Au@C and Au@SiO_2 are 153° and 34°, respectively. Carbon is a hydrophobic material, which can prevent acid in the aqueous solution from intruding into the carbon nanosphere support. Although silica is an inert and acid-resistant material, as a hydrophilic material it not only cannot prevent acid from intruding into the support but oppositely good for acidic aqueous solution to get in. Given that the Au size and the composite structure are the same (TEM image of Au@SiO_2 is shown in Fig. S1), it can be concluded that the Au@C composite material has acid resistance due to the hydrophobicity of carbon.

We then tested the CO catalytic oxidation activity. The reaction device for the catalytic oxidation of CO by the catalyst is a fixed bed at atmospheric pressure. 30 mg of Au@C was placed in a quartz tube. The reaction tube and thermocouple were fixed together to control the reaction temperature. The gas selected for the CO catalytic reaction in this experiment is a mixed gas of 1%CO/21%O_2/78%N_2. Gas flow rate is 45 mL/min. Gas concentration of reactant and product were detected by Gas Chromatograph (GC9800, Shanghai Kechuang Co., Ltd). The CO conversion is calculated by Eq. (1):

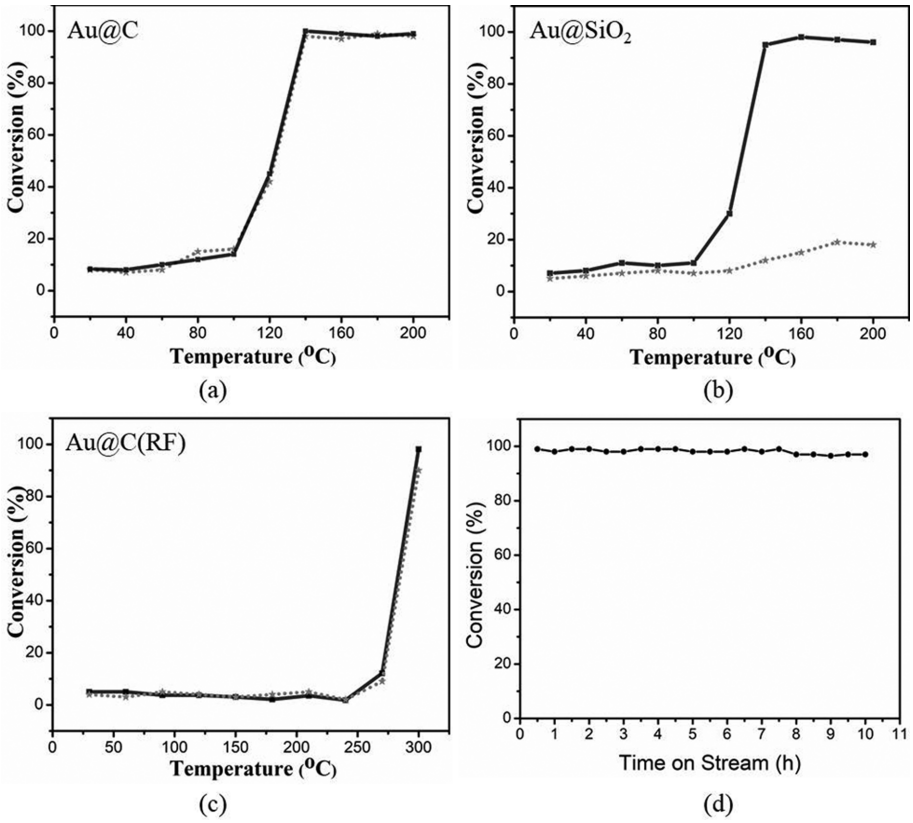

Fig. 5. The conversion of CO over (a) Au@C, (b) Au@SiO_2 and (c) Au@C(RF) at different temperatures before (solid line) and after (dotted line) acid resistance test. (d) Stability test of Au/C as a function of time on stream.

$$CO_{conversion}\% = \frac{[CO]_{in} - [CO]_{out}}{[CO]_{in}} \times 100\% \quad (1)$$

The CO_{in} and CO_{out} represent the CO gas concentration in the inlet and outlet, respectively. The catalytic properties of Au@C, Au@SiO_2, and Au@C(RF) before and after acid resistance test are shown in Fig. 5(a), (b), and (c), respectively. As can be seen, 100% CO conversion was obtained at 140 °C when we used Au@C catalyst and the activity was not affected by acid resistance tests, suggesting that the catalyst has both high activity and strong acid resistance. Carbon can only be eroded by high concentrations of strongly oxidizing acids, such as concentrated sulfuric or nitric acid, and the concentration and the oxidability of the acid under the reaction conditions here are not enough to corrode the carbon shell. However, when the reaction was catalyzed by Au@SiO_2, the catalytic activity decreased dramatically after acid etching, which can be attributed to the leaching of the active sites in acid media. Meanwhile, both the Au@C(RF) catalyst before and after acid etching showed the same low catalytic activity (the CO conversion reach 100% at 300 °C). That is because the size of Au in Au@C(RF) is larger (Fig. 2) due to the occurrence of aggregation in the absence of the anchoring of the amino groups.

The time-on-line activity was tested and shown in Fig. 5(d). It can be seen that the Au@C catalyst exhibited very high activity throughout the course of 10 h test. The carbon shell proved to be strong enough to endure long-term use. Besides, the high reaction temperature (140 °C) is high enough to avoid the accumulation of intermediate carbon species. Thus, the carbon shell would not be obstructive or damaged during the reaction.

In summary, Au nanoclusters coated by carbon were synthesized facilely via the reverse microemulsion-hydrothermal method. As a hydrophobic material, the carbon support ensures that the catalyst can maintain its activity in an acidic environment. The conversion of the composite catalyst can reach 100% at 140 °C. The Au@C catalyst has excellent acid resistance performance and has broad development prospects in the fields of CO oxidation removal in acid media.

ACKNOWLEDGEMENTS

The authors gratefully acknowledge the financial support of the Fundamental Research Funds for the Central Universities (No. DUT20JC31).

SUPPORTING INFORMATION

Additional information as noted in the text. This information is available via the Internet at http://www.springer.com/chemistry/journal/11814.

REFERENCES

1. M. Grätzel, *Chem. Lett.*, **34**, 8 (2004).

2. W. Yuan, C. Hou, X. Zhang, S. Zhong, Z. Luo, D. Mo, Y. Zhang and X. Liu, *ACS Appl. Mater. Interfaces*, **11**, 37626 (2019).
3. X. Xu, Z. Xia, X. Zhang, H. Li, S. Wang and G. Sun, *Nanoscale*, **12**, 3418 (2020).
4. G. Montiel, E. Fuentes-Quezada, M. M. Bruno, H. R. Corti and F. A. Viva, *RSC Adv.*, **10**, 30631 (2020).
5. D. Lee, S. Gok, Y. Kim, Y.-E. Sung, E. Lee, J.-H. Jang, J. Y. Hwang, O. J. Kwon and T. Lim, *ACS Appl. Mater. Interfaces*, **12**, 44588 (2020).
6. O. Tetsuya, M. Toshiyuki and T. Satoshi, *Chem. Lett.*, **35**, 10 (2006).
7. X. Lu, Z. Deng, C. Guo, W. Wang, S. Wei, S.-P. Ng, X. Chen, N. Ding, W. Guo and C.-M. L. Wu, *ACS Appl. Mater. Interfaces*, **8**, 12194 (2016).
8. N. Takezawa and N. Iwasa, *Catal. Today*, **36**, 45 (1997).
9. M. Haruta, T. Kobayashi, H. Sano and N. Yamada, *Chem. Lett.*, **16**, 405 (1987).
10. E. Quinet, L. Piccolo, F. Morfin, P. Avenier, F. Diehl, V. Caps and J.-L. Rousset, *J. Catal.*, **268**, 384 (2009).
11. Z. Wu, *Angew. Chem. Int. Ed.*, **51**, 2934 (2012).
12. M. Wang, Z. Wu, Z. Chu, J. Yang and C. Yao, *Chem. Asian J.*, **9**, 1006 (2014).
13. C. Aydin, J. Lu, N. D. Browning and B. C. Gates, *Angew. Chem. Int. Ed.*, **51**, 5929 (2012).
14. Y. Tao, M. Li, J. Ren and X. Qu, *Chem. Soc. Rev.*, **44**, 8636 (2015).
15. M. A. Tofanelli, K. Salorinne, T. W. Ni, S. Malola, B. Newell, B. Phillips, H. Häkkinen and C. J. Ackerson, *Chem. Sci.*, **7**, 1882 (2016).
16. N. Xia, Z. Gan, L. Liao, S. Zhuang and Z. Wu, *Chem. Commun.*, **53**, 11646 (2017).
17. J. Wang, Y. Zhao, W.-H. Wang and M. Bao, *Funct. Mater. Lett.*, **11**, 1850016 (2018).
18. J. Wang, X. Li, L. Luo, S. Zhang and R. Lu, *Ceram. Int.*, **39**, 9293 (2013).
19. H. Ye, J. Wang, W.-H. Wang and M. Bao, *Funct. Mater. Lett.*, **11**, 1850081 (2018).
20. J. Wang, Z. H. Shah, S. Zhang and R. Lu, *Nanoscale*, **6**, 4418 (2014).
21. J. Wang, X. Li, S. Zhang and R. Lu, *Nanoscale*, **5**, 4823 (2013).
22. Q. Yang, J. Wang, W.-H. Wang and M. Bao, *RSC Adv.*, **9**, 21473 (2019).
23. J. Wang, H. Jin, W.-H. Wang, Y. Zhao, Y. Li and M. Bao, *ACS Appl. Mater. Interfaces*, **12**, 19581 (2020).
24. H. Zhang, M. Yu, H. Song, O. Noonan, J. Zhang, Y. Yang, L. Zhou and C. Yu, *Chem. Mater.*, **27**, 6297 (2015).
25. J. Wang, W. Wu, Q. Yang, W.-H. Wang and M. Bao, *Funct. Mater. Lett.*, **11**, 1850003 (2018).
26. H. Jin, J. Wang, W.-H. Wang, Y. Li and M. Bao, *Catal. Commun.*, **141**, 106013 (2020).

Supporting Information

Facile construction of acid-resistant Au nanoclusters via hydrophobic carbon coating for catalyzing CO oxidation in acidic media

Hao Wang, Hong Liu, and Jiasheng Wang†

School of Chemical Engineering, Dalian University of Technology, Panjin 124221, China
(*Received 6 October 2021 • Revised 9 December 2021 • Accepted 2 January 2022*)

Section S1: Experimental Procedures

Materials:

Para-aminophenol (4-AR), resorcinol, and formaldehyde (aqueous solution with 37 wt% formaldehyde and 0.6 wt% of methanol) were purchased from the Macklin. Polyoxyethylene (5) nonylphenyl ether (NP-5) was obtained from the Sigma-Aldrich. Cyclohexane, ethanol, $HAuCl_4$, tetraethyl orthosilicate (TEOS), concentrated hydrochloric acid (36-38%), and aqueous ammonia (NH_4OH, 25-29%) were purchased from the Sinopharm Chemical Reagent Co., Ltd. The mixed gas of 1%CO/21%O_2/78%N_2 was purchased from Yingkou Jiahe Gas Co., LTD. All chemicals were used as received without any further purification.

Characterization:

Scanning electron microscopy (SEM) was carried out on FEI Nova 450 Nano SEM.

Transmission electron microscopy (TEM) analyses and high-resolution transmission electron microscopy (HRTEM) were carried out on FEI TecnaiG2 F30 equipment operating at 200 kV. The samples for TEM analysis were prepared by dispersing the products in the ethanol/water (3/1 volume ratio) solutions with sonication. The obtained mixture was dropped on the carbon-coated copper grids and dried at room temperature.

The pore channel information was gained from N_2 sorption by automatic physical adsorption analyzer (Quantachrome Instruments, Autosorb-iQ-C) at 77 K. The pore size was studied by Horvath-Kawazoe (HK) method.

The water contact angles (CA) were measured with a 5 μL DI water droplet by CA measurement (OCAH200, Dataphysics Instruments) with a CCD camera. The average CA value for the same sample was obtained by measuring more than three different positions.

Section S2

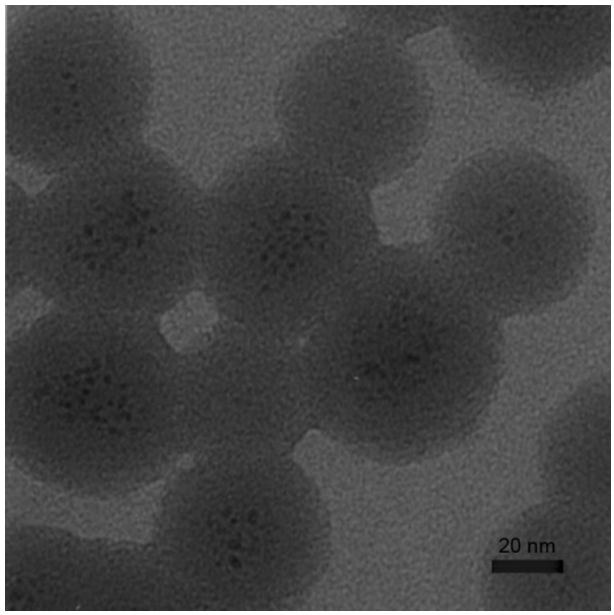

Fig. S1. TEM image of Au@SiO_2.